JACC Vol. 21, No. 3
March 1, 1993:743–53

A New Integrated System for Three-Dimensional Echocardiographic Reconstruction: Development and Validation for Ventricular Volume With Application in Human Subjects

MARK D. HANDSCHUMACHER, BS, JEAN-PAUL LETHOR, MD, SAMUEL C. SIU, MD, DONATO MELE, MD, J. MIGUEL RIVERA, MD, MICHAEL H. PICARD, MD, FACC, ARTHUR E. WEYMAN, MD, FACC, ROBERT A. LEVINE, MD, FACC

Boston, Massachusetts

Objectives. **The purpose of this study was to improve three-dimensional echocardiographic reconstruction by developing an automated mechanism for integrating spark gap locating data with corresponding images in real time and to validate use of this mechanism for the measurement of left ventricular volume.**

Background. **Initial approaches to three-dimensional echocardiographic reconstruction were often limited by inefficient reconstructive processes requiring manual coordination of two-dimensional images and corresponding spatial locating data.**

Methods. **In this system, a single computer overlays the binary-encoded positional data on the two-dimensional echocardiographic image, which is then recorded on videotape. The same system allows images to be digitized, traced, analyzed and displayed in three dimensions. This system was validated by using it to reconstruct 11 ventricular phantoms (19 to 271 ml) and 11 gel-filled excised ventricles (21 to 236 ml) imaged in intersecting long- and short-axis views and by apical rotation. To measure cavity volume, a surface was generated by an algorithm that takes advantage of the full three-dimensional data set.**

Results. **Reconstructed cavity volumes agreed well with actual values: $y = 0.96x + 2.2$ for the ventricular phantoms in long- and short-axis views ($r = 0.99$, SEE = 2.7 ml); $y = 0.95x + 2.9$ for the phantoms, reconstructed by apical rotation ($r = 0.99$, SEE = 2.7 ml); and $y = 0.99x + 0.11$ ml for the excised ventricles (reconstructed in long- and short-axis views; $r = 0.99$, SEE = 5.9 ml). The mean difference between three-dimensional and actual volumes was 3% of the mean (3.0 ml) for the phantoms and 6% (4.6 ml) for the excised ventricles. Observer variability was 2.3% for the phantoms and 5.6% for the excised ventricles. Application to 14 normal subjects demonstrated feasibility of left ventricular reconstruction, which provided values for stroke volume that agreed well with an independent Doppler measure ($y = 0.97x + 0.94$; $r = 0.95$, SEE = 3.2 ml), with an observer variability of 4.9% (2.4 ml).**

Conclusions. **A system has therefore been developed that automatically integrates locating and imaging data in no more time than the component two-dimensional echocardiographic scans. This system can accurately reconstruct ventricular volumes in vitro over a wide range and is feasible in vivo, thus laying the foundation for further applications. It has increased the efficiency of three-dimensional reconstruction and enhanced our ability to address clinical and research questions with this technique.**

(J Am Coll Cardiol 1993;21:743–53)

Current echocardiographic devices provide only two-dimensional tomographic views of the heart; to appreciate three-dimensional structural relations requires mental reconstruction of these views by an experienced observer. While this process may be satisfactory for structures of known and regular shape, it limits the ability to analyze structures of unknown or complex shape. In addition, quantitative measures of cardiac chamber size and performance, such as ejection fraction, must be derived from two-dimensional data subject to geometric assumptions. Three-dimensional reconstruction could eliminate the need for such assumptions and thereby facilitate accurate evaluation of chamber size and shape, ventricular function and complex congenital heart defects. It would also allow quantitative description of structures whose surfaces do not form enclosed volumes (such as valve leaflets), structures for which simple geometric models are less applicable (such as the right ventricle and ischemic left ventricle) and intracardiac flow fields from Doppler color flow images. However, to achieve these goals requires a method for registering the spatial location of multiple two-dimensional images and combining

From the Cardiac Ultrasound Laboratory, Massachusetts General Hospital, Department of Medicine, Harvard Medical School, Boston, Massachusetts. This study was supported in part by Grants HL-07535 and HL-38176 from the National Heart, Lung, and Blood Institute, National Institutes of Health, Bethesda, Maryland and by a grant from the Whitaker Foundation, Mechanicsburg, Pennsylvania. Dr. Lethor was supported by a grant from the Foundation de France and the Federation Francaise de Cardiologie, Paris, France. Dr. Siu was supported by Research Awards of the Alberta Heritage Foundation for Medical Research, Edmonton, Alberta, and the Medical Research Council of Canada, Ottawa, Ontario, Canada. Dr. Mele was supported in part by Academia delle Scienze, Ferrara, Italy. Dr. Levine is an Established Investigator of the American Heart Association, Dallas, Texas, with funds contributed in part by its Massachusetts Affiliate, Needham.

Manuscript received December 30, 1991, revised manuscript received and accepted August 14, 1992.

Address for correspondence: Robert A. Levine, MD, Cardiac Ultrasound Laboratory, Founders House 8, Massachusetts General Hospital, Boston, Massachusetts 02114.

0735-1097/93/$6.00

them in three dimensions at one or more points in the cardiac cycle.

Although the feasibility of initial reconstructive approaches has been demonstrated in the research environment (1–14), their application to larger populations has been restricted by the time-consuming process of coordinating images with their spatial locations. Most techniques slowly acquire individual images and their three-dimensional locations at discrete, sequential points in time and are therefore subject to potential inaccuracies caused by patient motion and respiration between images. In a previous study (15), a system was developed that could minimize these inaccuracies by continuously acquiring multiple views within a short period of time. However, such a system generates large numbers of images that must then be coordinated with their corresponding positions. As initially implemented, this requires manual coordination of images digitized by one computer with spatial locations from a separate computer based on their acquisition time during the scanning sequence. A third computer is then required to reconstruct and display the images in a three-dimensional format (Fig. 1A). This process is prohibitively long, particularly for dynamic reconstructions throughout the cardiac cycle. The data sets, once integrated, also require considerable computer storage.

The purpose of this study, therefore, was to develop and validate a fully integrated system for three-dimensional reconstruction towards the ultimate goal of applying this technique more readily and widely to evaluate cardiac structure and function. In particular, this system required the development of a mechanism for automated integration of images and positional data in real time, with recording of the combined data sets on videotape to provide convenient, high capacity data storage and retrieval. Real time data integration was achieved by interfacing both the two-dimensional imaging system and the spatial locating device to a single computer that overlays the positional data in binary format on an unused portion of the imaging signal and records the composite on videotape (Fig. 1B). This mechanism allows acquisition of spatially registered data during the routine echocardiographic examination, with time and storage requirements no greater than those for the component two-dimensional scans. This integrated system includes mechanisms for tracing, display and analysis of structures of interest in a three-dimensional format. It also uses a new algorithm developed to reconstruct surfaces from intersecting, nonparallel images to take full advantage of the ability to acquire multiple overlapping views from any tomographic orientation. This system was validated by demonstrating its ability to provide accurate volumetric reconstructions of objects and ventricles of known size and shape in vitro. This validation also lays the foundation for further applications. Initial feasibility in human studies was explored by applying this technique in 14 normal subjects to demonstrate its ability to reconstruct the left ventricle and to provide a quantitative measure of stroke volume that agrees well with an independent noninvasive measure by Doppler echocardiography. By increasing the efficiency of reconstruction, this system now provides a practically useful mechanism that should enhance our ability to address clinical and research questions with this technique.

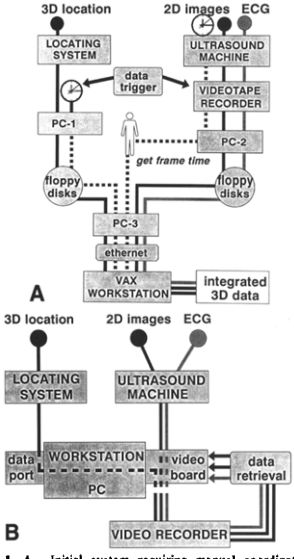

Figure 1. A, Initial system requiring manual coordination of images and spatial locations. During the scan, two-dimensional (2D) images and electrocardiogram (ECG) would be recorded on videotape along with a trigger signal that indicates the beginning of three-dimensional (3D) positional data collection by one personal computer (PC-1). Selected images were later digitized by another computer (PC-2). To coordinate each image with its corresponding spatial location, it was necessary to read the value of the frame counter from the image itself and manually enter it into a computer file. The offset of each frame from the trigger signal was then used to calculate the time in the positional data collection and to select the correct transducer position. Because of the systems used, the images and positional data had to be manually transferred by floppy disks to a third computer (PC-3) that was connected by a high-speed ethernet link to a mainframe VAX workstation used for data integration and processing. **B,** Real-time data integration. A single computer (WORKSTATION PC) is interfaced to both the locating system and ultrasound machine by way of a data port and video processing board. The video board overlays the positional data on the imaging signal and records the composite on videotape. The same computer system is used for data retrieval and analysis.

Methods

Volumetric and Ventricular Studies

The ability of this three-dimensional system to provide accurate reconstructions was tested by comparing the reconstructed shape and volume of ventricular phantoms and gel-filled ventricles with their actual shapes and measured volumes. A series of scans were performed on each object by two different observers and independently reconstructed by each.

Phantom preparation. Eleven balloons were filled with a heated solution of 5% agarose in water to obtain a range of volumes between 19 and 271 ml. The agarose solidified on cooling to provide objects of known size and shape that could be imaged in a water bath with distinct acoustic interfaces that could be easily traced. Therefore, the accuracy of reconstruction could initially be tested without the difficulties associated with image interpretation in biologic structures. The objects had a variety of elliptic and pear-like shapes with localized rounded protrusions to test the fidelity of reconstruction.

Ventricular preparation. A total of 11 excised hearts (7 canine, 3 human, 1 bovine) were also studied to provide a range of shapes and volumes (21 to 236 ml). They were prepared by first removing the atria and the right ventricular myocardium. The aortic and mitral valves were sewn shut and the left ventricular chamber was filled by syringe with agarose as before. The amount of agarose relative to ventricular size was varied in different hearts to obtain a range of possible shapes (elliptic to more spheric) corresponding to different states of ventricular filling.

Data acquisition. Objects were scanned in a water bath with the 3.5-MHz transducer of a Hewlett-Packard phased array sector scanner (77020A) at 12- to 16-cm depth settings. The entire object was scanned in intersecting long- and short-axis views or by apical rotation with the goal of acquiring high quality images from different views to reconstruct features of interest. (The excised ventricles were scanned in long- and short-axis views because the narrow apexes of the smaller canine hearts made consistent apical scanning difficult.) The three-dimensional positions of the images were recorded automatically and in real time during the scan as described later.

Patient studies. Demonstrating the initial feasibility of ventricular reconstruction by this system could be done most simply and noninvasively in subjects not undergoing catheterization; therefore, the ability of the technique to measure left ventricular stroke volume was assessed by comparing results with those of an independent noninvasive measure, the pulsed Doppler stroke volume, which has been extensively validated against other standards both experimentally and clinically (16–28). A total of 14 normal subjects were scanned in the left lateral decubitus position with the 3.5-MHz transducer of a Hewlett-Packard phased array sector scanner (77020A) with attached spark gap acoustic locating devices (2,6,15). This system permitted unrestricted scanning in two-dimensional views that were obtained during one quiet end-expiration period (roughly 20 to 30 s). Views were obtained by apical rotation or as intersecting parasternal long- and short-axis views, depending on which images were optimal. Images were recorded on videotape with a system that overlays binary-encoded positional data on an unused portion of the video signal in real time. Two-dimensional views and Doppler spectra needed to calculate stroke volume were obtained immediately after the scan, with the patient in the same body position and at the same phase of respiration (see later). Informed consent of the subjects (10 men and 4 women, aged 23 to 31 years) had been obtained for noninvasive imaging, as approved by the institutional Human Studies Review Board.

Doppler studies. Stroke volume across the aortic valve was calculated by multiplying the cross-sectional area at the level of the aortic anulus by the time-velocity integral of flow across that valve. Area was calculated from the peak diameter at the insertion of the aortic valve leaflets in the parasternal long-axis view, assuming a circular configuration (23,24,26–28). Outflow velocities were obtained by pulsed Doppler echocardiography from the apex with the sample volume at the level of the measured diameter and scanned radially to provide optimal alignment with flow. The time-velocity integral was calculated by tracing the modal velocity (darkest portion of the velocity spectrum, representing the greatest number of scatterers) and averaging over 5 beats. The product of area and time-velocity integral provided stroke volume (16,17,23,24,26–28). Mitral stroke volume was calculated by the method of Fisher et al. (19) as the product of peak mitral valve cross-sectional area at the level of the leaflet tips from the parasternal short-axis view times the mean/maximum ratio of mitral valve excursion from an M-mode tracing at that level times the time-velocity integral of modal velocity at the level of the leaflet tips by pulsed Doppler echocardiography in the apical four-chamber view (mean of 5 beats) (19–21,23–26,28). The mean of aortic and mitral stroke volumes was used to strengthen the estimate (28). No patient had mitral or aortic regurgitation or stenosis. (Observer variability of these measures has been reported to be <7% by our group and others [29,30].)

Reconstruction Technique

Transducer localization. The position of the ultrasound image in space was determined by using three spark gap locating devices that bear a fixed relation to the plane of the sector scan (2,6,15). These devices are located on a plate perpendicular to the long-axis of the transducer; the plate is mounted on a Plexiglas sleeve reproducibly fixed to the transducer (Fig. 2A). Each spark gap emits audible sound toward an array of microphones that time the arrival of sound and determine the spark gap location by triangulation. A square array of four microphones is used that provides several calculations for internal consistency; the array is mounted on a heavy tripod for stability. This spark gap

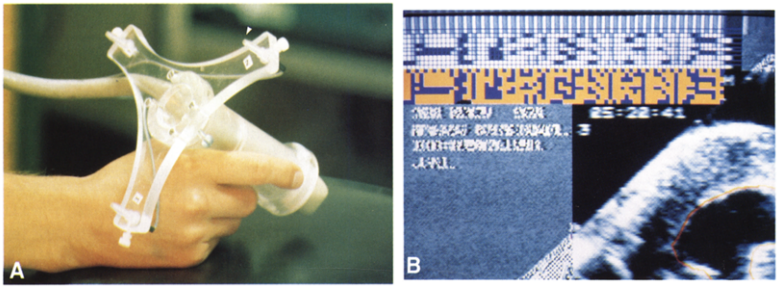

geometry provides accurate data from a wide range of views without interfering with the ultrasound operator.

The three spark gaps are fired in rapid succession by a microprocessor (Science Accessories). Each time the three spark gaps are fired (30 times/s), the transducer location can be calculated. Because the transducer may move slightly between spark gap firings, their locations are taken as the least-squares fit to their known positions on the Plexiglas plate. Deviations from the known distances between spark gaps, indicating rapid transducer motion or obstruction of the acoustic path, lead to exclusion of that data set. This system improves on the one previously described (15) by 1) using a larger distance between spark gaps (14 cm) to improve precision, and 2) using a parallel data port (P11P, Science Accessories) in the microprocessor connections to provide roughly 30 positions/s rather than only 10, thereby updating position at a rate comparable to that of video frame acquisition.

Figure 2 (above). A, Ultrasound transducer with three spark gaps (**arrowhead**) mounted parallel to its long axis; this configuration provides direct transmission of audible sound toward the localizing microphone array. B, Expanded view of a recorded image showing the digitally encoded positional data in black and white (**upper left**); the computer has decoded this information and displayed it in color below the recorded pattern. The **central box** shows the portion of the ultrasound image that is stored; in this case it shows a short-axis view of a canine left ventricle with superimpesed endocardial trace in color. Each bit of binary data is represented as a 4×4 pixel region of high or low intensity positioned on the image using x and y pixel coordinates provided to the video processing board. When this pattern is subsequently digitized from video, the data are decoded based upon their defined positions on the image.

Figure 3 (below). Gel-filled ventricular phantom (**A**) with reconstructed traces acquired in long- and short-axis views (**B**) and the calculated surface (**C**), demonstrating reproduction of shape (body and protuberance).

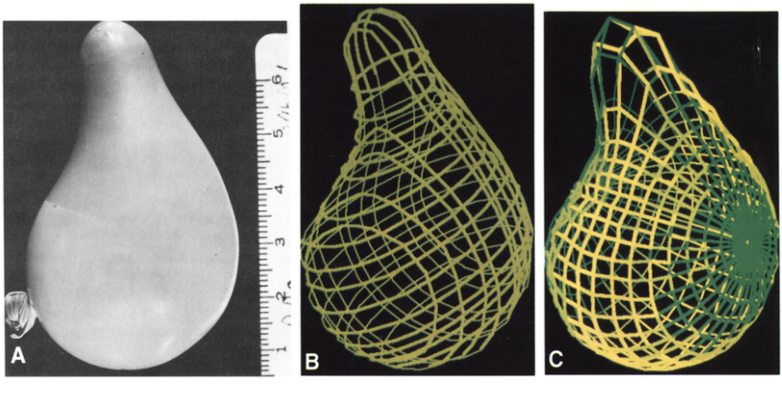

System description. A single 386-series personal computer (SUN 386i, Sun Microsystems) is interfaced to both the transducer-locating system and the ultrasound machine by means of a high speed data port (PIO-12 MetraByte) and a special purpose video processing board (AT Vista, TrueVision) that are added to expansion slots on the computer bus (Fig. 1B). At any desired point within an ultrasound scan, this computer can initiate continuous spark gap firing and receive positional data by way of the data port. Each time positional data is received from the locating system, it is sent to the video board and encoded as a binary pattern that is overlaid on an unused portion of the video signal that comes directly from the ultrasound machine. The composite video signal is then recorded in real time on videotape (Fig. 2B). The digital overlay consists of six data lines that correspond to the two most recent positions of each of the three spark gaps. Recording the two most recent locations with each image allows the magnitude of transducer motion to be calculated from that image alone, so that frames acquired during rapid motion can be excluded to improve the accuracy of the reconstruction. The software was optimized so that the overlay on each videoframe included two or three new spark gap positions obtained within the video frame time (33 ms). Every frame then contains all the raw data required for three-dimensional reconstruction (images, ECG and spatial information) so that manual alignment or coordination of these data is not required.

Data Analysis

Data retrieval from videotape. After scanning, the same system is used for data retrieval. Up to 30 different tomographic images/study could be selected from video playback by digitizing the video signal to produce 1) an image digitized with 486 × 756 spatial resolution and 8 bits of intensity resolution/pixel (only the central portion of the frame, corresponding to the echocardiographic data, was saved); and 2) decoded positional data from which the spark gap locations were calculated to derive a transformation matrix that positions each pixel correctly in three-dimensional space. Data decoding and matrix calculation required <1 s/image.

Border definition. To reconstruct a ventricular surface, the digitized images were traced on a graphics screen by using a digital pointing device incorporated into the same system. The reconstruction and surfacing algorithms were specifically designed to tolerate incomplete traces so that portions of images that are difficult to interpret (because of partial view or lateral dropout) can remain untraced and can be filled in from intersecting views and other windows. At any point during tracing, the consistency of border identification could be checked by quickly paging through the two-dimensional images with overlaid traces and simultaneously displaying the current trace in its spatial relation to all the others. Appreciating three-dimensional relations could be improved by dynamically rotating the composite with depth cuing and optional stereo visualization. Any selected trace could then be retraced for best alignment with intersecting borders. The central portion of the two-dimensional echocardiographic border reflections were traced because 1) this would, in principle, correspond to the border of the object intersected by the *central plane* of the ultrasound sector, where the tracing is positioned by the three-dimensional system (the thickness of the reflection being produced by a beam of finite out of plane width intersecting a generally curved surface); and 2) in a series of pilot studies, this provided the closest correspondence with actual volumes (within ±3% of actual volumes in three initial hearts, as opposed to consistent under- or overestimation of up to 10% by tracing the inner or outer borders of the reflection). Tracing typically required 10 to 30 min depending on observer experience, the number of images (15 to 30) and their complexity.

Surfacing algorithm. Previous surfacing algorithms have often fitted data to curves in a series of parallel *two-dimensional* planes and then simply extrapolated between these slices to create an enclosed surface. To include the full strength of *intersecting three-dimensional data* in the basic fitting process, a new approach was devised. An initially spheric template, positioned at the geometric center of the cavity, was deformed to provide the best fit to surrounding traces. It was divided into evenly spaced lines of latitude and longitude to provide ≈500 grid points. Rays were then extended from the center of the sphere through these grid points toward the traced borders to calculate a corresponding grid point on the ventricular surface. The position of this point was obtained as a best fit to all traced line segments within a small conical sector (10.6°) around each ray, weighted by their proximity to the ray. Values for rays without adjacent traces were filled in by interpolating between nearest neighbors. The grid points were then connected and the surface displayed.

Volume calculation. Cavity volume was calculated by treating the surface as a series of contiguous triangular patches of grid points, each forming (with its attached rays) a tetrahedron with its apex at the center of the cavity. The volumes of these figures were summed and compared with the actual volumes of the agarose casts determined by water displacement in a graduated beaker. For the excised ventricles, the myocardium was incised and carefully peeled off the agarose cast, which was then measured.

Analysis of patient studies. For each view, end-diastolic and end-systolic images (largest and smallest cavity size) were selected by two independent observers, and endocardial borders traced using a digital pointing device. End-diastolic and end-systolic cavity volumes were then calculated by applying the surfacing algorithm, and stroke volume calculated as their difference.

Statistical analysis. The accuracy of the reconstructed volume was examined by 1) linear regression of calculated versus actual volumes for each observer; and 2) calculation of the absolute difference between calculated and actual volumes for each observer. Observer variability was expressed as the standard deviation of the differences between

the measurements of the two observers for both the in vitro and the in vivo studies.

Results

Ventricular phantoms. The reconstructed traces and derived surfaces reproduced the shape of the scanned objects (Fig. 3). Reconstructed cavity volumes agreed well with actual values. For reconstructions in *long- and short-axis views*, linear regression gave $y = 0.96x + 2.2$ for the pooled data of both observers ($r = 0.99$, SEE = 2.7 ml) (Fig. 4, top). (Individual results were $y = 0.97x + 1.5$ for one observer [$r = 0.99$, SEE = 2.7 ml] and $y = 0.95x + 2.9$ for the other [$r = 0.99$, SEE = 2.4 ml].) For the *apical rotations*, linear regression gave $y = 0.95x + 2.9$ for both observers ($r = 0.99$, SEE = 2.7 ml) (Fig. 4, middle). (Individual results were $y = 0.97x + 2.3$ for one observer [$r = 0.99$, SEE = 2.3 ml] and $y = 0.94x + 3.5$ for the other [$r = 0.99$, SEE = 2.0 ml].) The mean difference between three-dimensional and actual volumes was 2.5% of the mean (3.0 ml), and observer variability was 2.3% of the mean (2.6 ml) (similar for both scan techniques).

Excised ventricles. The reconstructions reproduced the shapes and important morphologic features of the actual ventricles. Figure 5 shows a reconstructed canine heart, with evident outflow tract, apex and papillary muscle indentations. Figure 6 shows how the reconstruction reproduced an apical aneurysm in a human heart compared with the agarose cast of that heart. Calculated volumes agreed well with actual values: $y = 0.99x + 0.11$ for the pooled data of both observers ($r = 0.99$, SEE = 5.9 ml) (Fig. 4, bottom). (Individual results were $y = 0.98x - 1.2$ for one observer [$r = 0.99$, SEE = 4.4 ml] and $y = 1.0x + 1.4$ for the other [$r = 0.99$, SEE = 6.7 ml].) Even if the largest two ventricles were excluded, leaving ventricles of <100 ml, correlations were virtually unchanged: $y = 0.99x + 0.02$ ($r = 0.98$, SEE = 4.6 ml) for the two observers, with $r = 0.98 - 0.99$ for each observer alone. The mean difference between three-dimensional and actual volumes was 6% of the mean (4.6 ml). Observer variability was 5.6% of the mean (4.3 ml).

In vivo ventricular reconstruction. In all 14 subjects, coherent endocardial surfaces could be generated from the views obtained. Figure 7A, for example, shows one of these ventricles reconstructed from a series of apical views in systole, illustrating the relation of the ventricle to adjacent atrial and aortic structures, a papillary muscle indentation along its inferior surface, and the curvature of the mitral anulus region at the atrioventricular junction. Systolic and diastolic traces can also be superimposed, as in Figure 7B. Figure 8 shows how intersecting apical (in this case, para-apical long-axis) and parasternal views can be combined to provide a three-dimensional reconstruction in another subject.

Stroke volume. Three-dimensional and Doppler stroke volume values agreed well (Fig. 9, Table 1, $y = 0.97x + 0.94$; $r = 0.95$, SEE = 3.2 ml by linear regression). The mean difference between the two values was 2.1 ml, or 4.3% of the mean. Observer variability was 4.1 ml, or 6.4% of the mean value, for volume (end-diastolic and end-systolic) and 2.4 ml, or 4.9% of the mean, for stroke volume.

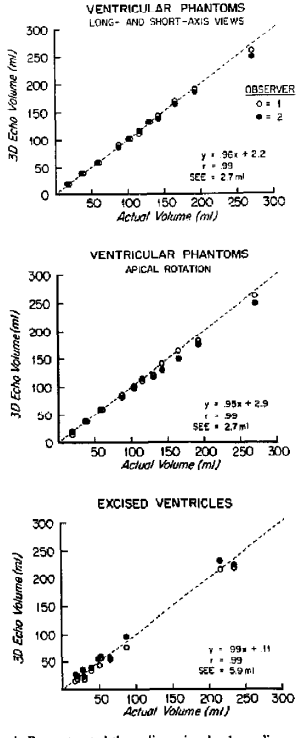

Figure 4. Reconstructed three-dimensional echocardiographic (3D Echo) volumes versus actual volumes plotted for two observers and compared with the line of identity. Linear regression results are given for the pooled data of both observers.

Discussion

Three-dimensional reconstruction: limitations of existing methods. Noninvasive three-dimensional reconstruction of cardiac structures has been a long-standing but prac-

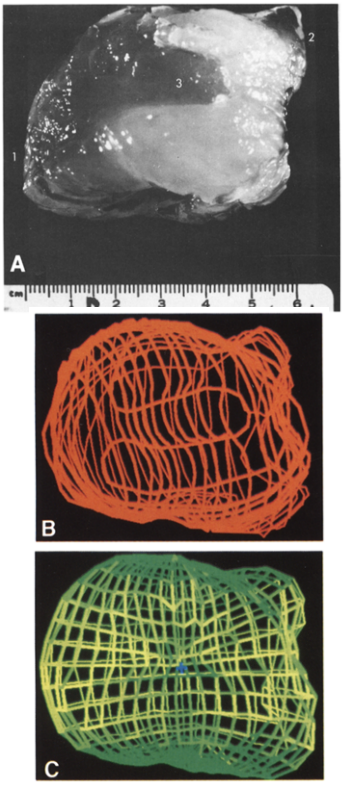

Figure 5. Agarose cast of a canine left ventricle (**A**) showing apex (1), outflow tract (2) and papillary muscle indentation (3). These features are reproduced in the reconstruction (**B**), which has been rotated several degrees to provide a better appreciation of the intersecting traces. The calculated surface is shown in **C**. (The endocardial border is being viewed in each case, and the surfacing algorithm, by its nature, may tend to smooth out certain features without altering net volume.)

tically elusive goal of echocardiographic imaging. Potential benefits include improved appreciation of three-dimensional spatial relations in valvular and congenital heart disease and improved measures of chamber volume and contractile function. These measures are particularly important in ischemic heart disease, in which two-dimensional methods based on geometric assumptions are most prone to error from distorted geometry and regional dysfunction. Although previous studies have demonstrated the feasibility of reconstructing cardiac structures in three dimensions, they have been limited to small numbers of individuals by several factors: 1) Some approaches demand views that conform to a predetermined geometry of reconstruction (4,8–10,12,14). Parallel slice techniques are most applicable to the open chest situation, whereas fixed point techniques may not always provide uniformly adequate echocardiographic views or visualize the entire chamber of interest from a single window. 2) Most techniques acquire individual images and their spatial locations at discrete, sequential points in time (1–9,13) and are therefore subject to potential inaccuracies caused by patient motion and respiration between images. 3) Continuous, rapid acquisition of multiple, unrestricted views overcomes the preceding limitations but magnifies the problem of coordinating large numbers of images with their corresponding positional data. In previous studies (31), this proved to be a rate-limiting manual step that became prohibitively long, particularly for dynamic reconstructions at multiple points within the cardiac cycle.

Integrated system. The present study validates a system developed to overcome the above limitations with the ultimate goal of realizing the full potential of three-dimensional reconstruction in more widespread applications. This system integrates into a single workstation all the components necessary for routine three-dimensional reconstruction. It automates the process of coordinating images and locating data acquired continuously and provides convenient, high volume storage in a videotape format. This system can therefore acquire all the data needed for three-dimensional reconstruction with time and storage requirements no greater than those of the component two-dimensional scans. Continuous acquisition of multiple views permits structures of interest to be scanned rapidly, minimizing problems of patient motion and respiration; at the same time, the previous rate-limiting steps required for data coordination have been eliminated. Convenience of data analysis is also provided by a unified system that permits data retrieval, tracing of structures of interest, three-dimensional display and calculation of surfaces with enclosed volumes. Digital data can also be acquired on-line as permitted by computer memory.

Ventricular reconstruction. The results of this study demonstrate that such a system can accurately reconstruct excised ventricles and ventricular phantoms with a wide range of shapes and sizes, reproducing localized protuberances, papillary muscle indentations and a left ventricular aneurysm. Correlations with directly measured volumes were good and the absolute differences between reconstructed and actual volumes were acceptably small, averaging 3.0 ml for the phantoms and 4.6 ml for the excised ventricles, with comparable observer variability. Although

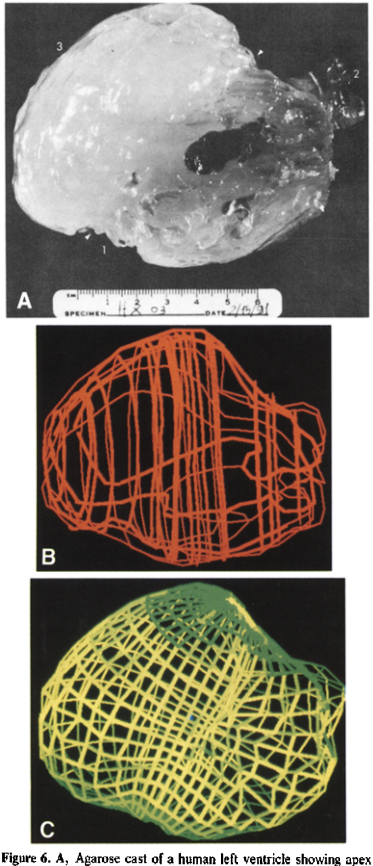

Figure 6. A, Agarose cast of a human left ventricle showing apex (1), outflow tract (2) and large anteroapical aneurysm (3), demarcated by arrows. These features are reproduced in the reconstructed traces (**B**). The calculated surface is shown in **C**.

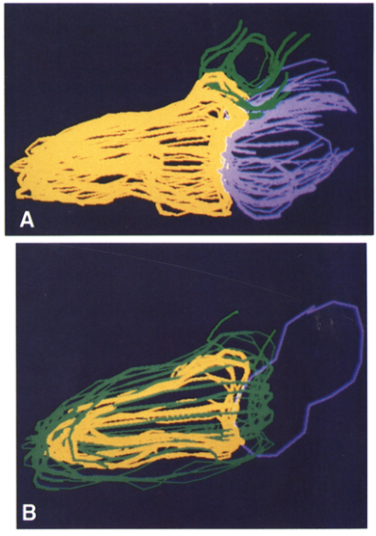

Figure 7. A, Normal human left ventricle reconstructed from apical views in vivo at peak systolic contraction. The endocardial border is shown in yellow with the apex to the left. The left atrium is traced in blue and the aortic root in green. A papillary muscle indentation can be seen along the inferior surface of the ventricle, and the curvature of the mitral ring is evident at the atrioventricular junction. **B,** Superimposed endocardial borders in systole (yellow) and diastole in another subject. (The centers of the systolic and diastolic ventricular traces are superimposed.)

in vitro volumes can be calculated by other methods (2,6,10,14), these results validate the system described, which increases the efficiency of data acquisition and reconstruction; they serve as a foundation for its application to clinical and research questions. The results also show the initial feasibility of applying this system in human subjects and its ability to provide a quantitative measure of left ventricular stroke volume that agrees well with an independent method based on flow. Data from multiple unrestricted imaging planes could, in fact, be rapidly acquired during one breath-holding period and reconstructed to provide a coherent surface. Freedom of transducer motion permitted acquisition to be adapted in the person being examined in order to optimize images, which could include both parasternal and apical or para-apical views.

Features promoting accuracy. One feature of the system contributing to this accuracy is the ability to review traces in three dimensions, using adjacent and intersecting images to improve border detection. This was particularly helpful for the excised ventricles, in which endocardial border definition was more difficult. Review of the reconstructed traces could readily detect misalignment between a poorly visualized border (affected, for example, by lateral drop-

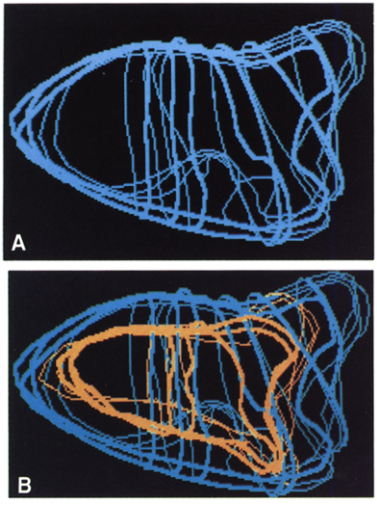

Figure 8. Left ventricle reconstructed from para-apical long-axis and parasternal short-axis views in vivo at end-diastole (**A**) and with peak systole superimposed (**B**).

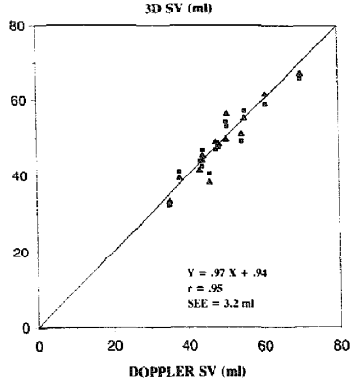

Figure 9. Three-dimensional (3D) versus Doppler stroke volume (SV) for the two observers (squares and triangles); the line of identity is shown.

out) and adjacent, better visualized borders. Such traces could be identified and corrected by paging through the individual two-dimensional images displayed beside the reconstruction, highlighting each trace in sequence. In vivo, border recognition was also facilitated by the availability of more than one image per cardiac cycle. Another important feature is the ability of the surfacing algorithm to accept partial (unclosed) traces. This allows use of views which do not include the entire structure of interest, and eliminates the need to complete traces in regions of poor border definition. Missing data can be filled in from intersecting views, from other windows, or by the surfacing algorithm itself, which bridges gaps between grid points in three dimensions. This reflects an advantage of an algorithm that achieves the best fit to data in three-dimensional regions, rather than fitting data to single curves in two-dimensional slices only.

Sources of variability. There are several sources of variability in the reconstruction, including 1) the resolution of spark-gap location (< 1 mm by selection of data sets to have the computed distances between spark gaps differ by no more than that amount from actual values); 2) ultrasound imaging resolution and the uncertainty created by the video rasterline spacing (digital scan conversion; in the millimeter range for axial resolution); and 3) observer variability (greater for tracing endocardial borders in the excised and in vivo ventricles). The results indicate these effects are acceptably small in the settings studied. In vivo, respiratory variability may need to be considered and possibly minimized by respiratory gating, although in a recent study, that did not appear to affect accuracy (12). In the human studies, we were able to obtain all the images needed to reconstruct the beating human left ventricle from scans during a single held

Table 1. Data From Human Studies

	Observer 1			Observer 2			Doppler
Pt No.	EDV	ESV	3D SV	EDV	ESV	3D SV	SV
1	113.1	47.1	66.0	109.5	42.2	67.3	70.1
2	56.9	24.6	32.3	60.5	27.1	33.4	35.0
3	97.0	42.7	54.3	94.2	44.4	49.8	50.3
4	131.8	78.7	53.1	131.4	74.9	56.5	50.6
5	96.2	39.1	57.1	97.0	41.5	55.5	55.2
6	63.2	22.7	40.5	59.8	21.6	38.2	45.8
7	80.2	32.6	47.6	85.6	37.0	48.6	48.4
8	77.7	30.8	46.9	79.8	30.8	49.0	47.6
9	77.9	31.2	46.7	69.9	24.4	45.5	44.0
10	90.2	41.0	49.2	90.8	39.6	51.2	54.4
11	100.3	41.3	59.0	101.7	39.9	61.8	60.8
12	75.7	33.2	42.5	85.6	41.3	44.3	43.9
13	80.8	36.9	43.9	77.2	35.6	41.6	43.2
14	86.7	45.6	41.1	85.5	46.1	39.4	37.7

All results are in ml. EDV = end-diastolic volume; ESV = end-systolic volume; Pt = patient; SV = stroke volume; 3D = three-dimensional echocardiography.

expiration (roughly 20 to 30 s) (Fig. 7 and 8). This takes advantage of the ability of the system to acquire views rapidly and continuously with automated spatial registration, thereby eliminating the effect of respiratory motion.

Future work. Transducers providing two simultaneous orthogonal views (32) or multiple views by phased-array parallel processing (33) should make image acquisition even faster. With improved efficiency of *acquisition* in this system, endocardial border detection has become the most time-consuming step, particularly in reconstructing more than one point in the cardiac cycle; this could affect implementation and clinical acceptance. This concern could potentially be overcome by defining the minimal number of views required (4) and by using new systems for on-line or off-line border detection based on signal amplitude or the presence of flow to automate or semi-automate border extraction with the option of manual editing. Such systems could be particularly strengthened by the availability of a three-dimensional data set that can bridge over gaps in individual two-dimensional images using minimal-cost functions that optimize the detection of a spatial border (34). Regarding dynamic reconstructions, tracing a second time point (for example, diastole) in a given view takes considerably less time than tracing the initial image (for example, systole) because of increasing familiarity with the view. In addition, analyzing multiple time points can be facilitated by techniques that, given one initial trace, apply optical flow tracking and simulated annealing techniques of matching corresponding contours to define borders automatically throughout the rest of the cardiac cycle (35–39). (Although decreased noise in many magnetic resonance images favors automated border extraction, the differentiation of relatively stagnant blood pool from myocardium on standard images can be most difficult in patients with ischemic or myopathic dysfunction, in whom functional evaluation is of greatest importance. Respiration and patient motion must also be considered in reconstruction by nuclear magnetic resonance imaging, which, in its conventional form, acquires images over multiple cardiac cycles. Echocardiographic systems, including the current one, have the added advantages of portability and lower equipment cost.)

Summary. We have developed a system that allows us to integrate images and positional data automatically, with time and storage requirements that are no more than those for an ordinary two-dimensional echocardiographic study. Data for three-dimensional reconstruction can therefore be obtained during a routine echocardiographic examination. This mechanism greatly simplifies the process of subsequent tracing and reconstruction. The system also integrates the capabilities for tracing features and deriving continuous surfaces from them to permit quantitative analysis using the full strength of the three-dimensional data set. We have shown that such a system can accurately reconstruct simple objects as well as ventricles of known size and shape. In addition, rapid acquisition of three-dimensional echocardiographic data and quantitative volumetric reconstruction of the left ventricle in human subjects are both feasible and provide a stroke volume that agrees well with independently measured values. The increased efficiency of data acquisition and reconstruction provided by this system should enhance the applicability of three-dimensional reconstruction to clinical and research questions at this time; the validation studies lay the foundation for such applications.

We thank John Newell for his elegant solution for tetrahedral volume, Iain Wright for his skillful construction of the spark gap mounting and microphone array and Sheila McGinty for her expert secretarial assistance.

References

1. Geiser EA, Ariet M, Conetta DA, Lupkiewicz SM, Christie LG, Conti CR. Dynamic three-dimensional echocardiographic reconstruction of the intact human left ventricle: technique and initial observations in patients. Am Heart J 1982;103:1056–65.
2. Moritz WE, Pearlman AS, McCabe DH, Medema DK, Ainsworth ME, Boles MS. An ultrasonic technique for imaging the ventricle in three dimensions and calculating its volume. IEEE Trans Biomed Eng 1983; BME-30:482–91.
3. Nixon JV, Saffer SI, Lipscomb K, Blomqvist CG. Three-dimensional echoventriculography. Am Heart J 1983;106:435–43.
4. Weiss JL, Eaton LW, Kallman CH, Maughan WL. Accuracy of volume determination by two-dimensional echocardiography: defining requirements under controlled conditions in the ejecting canine left ventricle. Circulation 1983;67:889–95.
5. Sawada H, Fujii J, Kato K, Onoe M, Kuno K. Three dimensional reconstruction of the left ventricle from multiple cross sectional echocardiograms: value for measuring left ventricular volume. Br Heart J 1983;50:438–42.
6. Linker DT, Moritz WE, Pearlman AS. A new three-dimensional echocardiographic method of right ventricular volume measurement: in vitro validation. J Am Coll Cardiol 1986;8:101–6.
7. Reichlen JS, Trivedi SS, Herman GT, St. John Sutton MG, Reichek N. Dynamic three-dimensional reconstruction of the left ventricle from two-dimensional echocardiograms. J Am Coll Cardiol 1986;8:364–70.
8. Sapoznikov D, Fine DG, Masseri M, Gotsman MS. Left ventricular shape, wall thickness, and function based on three-dimensional reconstruction echocardiography. Comput Cardiol 1987:495–8.
9. McCann HA, Chandrasekaran K, Hoffman EA, Sinak LJ, Kinter TM, Greenleaf JF. A method for three-dimensional ultrasonic imaging of the heart in vivo. Dynam Cardiovasc Imaging 1987;1:97–109.
10. Buckey JC, Beattie JM, Nixon JV, Gaffney FA, Blomqvist CG. Right and left ventricular volumes in-vitro by a new nongeometric method. Am J Card Imaging 1987;1:227–33.
11. Collins SM, Chandran KB, Skorton DJ. Three-dimensional cardiac imaging. Echocardiography 1988;5:311–9.
12. Zoghbi WA, Buckey JC, Massey MA, Blomqvist CG. Determination of left ventricular volumes with use of a new nongeometric echocardiographic method: clinical validation and potential application. J Am Coll Cardiol 1990;15:610–7.
13. King DL, King DL Jr, Shao MY. Three-dimensional spatial registration and interactive display of position and orientation of real-time ultrasound images. J Ultrasound Med 1990;9:525–32.
14. Mensah GA, Pini R, Mommini E, et al. Three-dimensional echocardiographic reconstruction: experimental validation of volume measurement (abstr). J Am Coll Cardiol 1991;17:291A.
15. Levine RA, Handschumacher MD, Sanfilippo AJ, et al. Three-dimensional echocardiographic reconstruction of the mitral valve, with implications for the diagnosis of mitral valve prolapse. Circulation 1989; 80:589–98.
16. Steingart RM, Meller J, Barovick J, Patterson R, Herman MV, Teichholz LE. Pulsed Doppler echocardiographic measurement of beat-to-beat changes in stroke volume in dogs. Circulation 1980;62:542–8.
17. Magnin PA, Stewart JA, Myers S, Kisslo JA. Combined Doppler and

phased-array echocardiographic estimation of cardiac output. Circulation 1981;63:388–92.

18. Lewis JF, Kuo LC, Nelson JC, Limacher MC, Quinones MA. Pulsed Doppler echocardiographic determination of stroke volume and cardiac output: clinical validation of two new methods using the apical window. Circulation 1984;70:425–31.
19. Fisher DC, Sahn DJ, Friedman JM, et al. The mitral valve orifice method for noninvasive two-dimensional echo Doppler determination of cardiac output. Circulation 1983;67:872–7.
20. Zhang Y, Nitter-Hauge S, Ihlen H, Myhre E. Doppler echocardiographic measurement of cardiac output using the mitral orifice method. Br Heart J 1985;53:130–6.
21. Hoit BD, Rashwan M, Watt C, Sahn DJ, Bhargava V. Calculating cardiac output from transmitral volume flow using Doppler and M-mode echocardiography. Am J Cardiol 1988;62:131–5.
22. Rokey R, Kuo LC, Zoghbi WA, Limacher MC, Quinones MA. Determination of left ventricular diastolic filling parameters with pulsed-Doppler echocardiography: comparison with cineangiography. Circulation 1985; 71:543–50.
23. Stewart WJ, Jiang L, Mich R, Pandian N, Guerrero JL, Weyman AE. Variable effects of changes in flow rate through the aortic, pulmonary and mitral valves on valve area and flow velocity: impact on quantitative Doppler flow calculations. J Am Coll Cardiol 1985;6:653–62.
24. Loeber CP, Goldberg SJ, Allen HD. Doppler echocardiographic comparison of flows distal to the four cardiac valves. J Am Coll Cardiol 1984;4:268–72.
25. Ascah KJ, Stewart WJ, Jiang L, et al. A Doppler two-dimensional echocardiographic method for quantitation of mitral regurgitation. Circulation 1985;72:377–83.
26. Rokey R, Sterling LL, Zoghbi WA, et al. Determination of regurgitant fraction in isolated mitral or aortic regurgitation by pulsed Doppler two-dimensional echocardiography. J Am Coll Cardiol 1986;7:1273–8.
27. Blumlein S, Bouchard A, Schiller NB, et al. Quantification of mitral regurgitation by Doppler echocardiography. Circulation 1986;74:306–14.
28. Labovitz AJ, Buckingham TA, Habermehl K, Nelson J, Kennedy HL, Williams GA. The effects of sampling site on the two-dimensional echo-Doppler determination of cardiac output. Am Heart J 1985;109:327–32.
29. Nicolosi GL, Pungercic E, Cervesato E, et al. Feasibility and variability of six methods for the echocardiographic and Doppler determination of cardiac output. Br Heart J 1988;59:299–303.
30. Chen C, Thomas JD, Anconina J, et al. Impact of impinging wall jet on color Doppler quantification of mitral regurgitation. Circulation 1991;84: 712–20.
31. Handschumacher MD, Sanfilippo AJ, Rodriguez L, Weyman AE, Levine RA. Dynamic three-dimensional echocardiographic reconstruction of the normal human mitral valve (abstr). Circulation 1990;82(suppl III):III-69.
32. Snyder JE, Kisslo J, von Ramm OT. Real-time orthogonal mode scanning of the heart. I. System design. J Am Coll Cardiol 1986;7:1279–85.
33. Sheikh KH, Smith SW, von Ramm OT, Kisslo J. Real-time, three-dimensional echocardiography: feasibility and initial use. Echocardiography 1991;8:119–25.
34. Thedens DR, Skorton DJ, Fleagle SR. A three-dimensional graph searching technique for cardiac border detection in sequential images and its application to magnetic resonance image data. Comput Cardiol 1991:57–60.
35. Zhang LF, Geiser DA. An effective algorithm for extracting serial endocardial borders from two-dimensional echocardiograms. IEEE Trans Biomed Eng 1984;31:441–7.
36. Friedland N, Adam D. Automatic ventricular cavity boundary detection from sequential ultrasound images using simulated annealing. IEEE Trans Med Imaging 1989;8:344–53.
37. Mailoux A Bleau, Bertrand M, Perticlere R. Computer analysis of heart motion from two-dimensional echocardiograms. IEEE Trans Biomed Eng 1987;34:356–64.
38. Duncan J, Owen R, Anandan P, et al. Shape-based tracking of left ventricular motion. Comput Cardiol 1991:41–4.
39. Friedland NS. Cavity boundary detection from sequential echocardiograms using a temporally adaptive multilevel energy function. Comput Cardiol 1991:427–30.